

EVALUATING TUNNEL JUNCTION BEHAVIOUR: A COMPARATIVE STUDY OF 3D AND 2D EQUIVALENT SPAN ANALYSES

Shenyan Yao
AECOM, Sydney, Australia

ABSTRACT

Tunnel junctions present greater geometric complexity than mainline tunnels, behaving in a three-dimensional (3D) manner under applied loads rather than conforming to two-dimensional (2D) plain strain conditions. While 3D modelling offers a more accurate representation of junction geometry, it is resource- and time-intensive and comparable outcomes can be achieved using representative 2D modelling. In recent Sydney tunnel projects, a simplified method has been adopted to estimate displacement and support performance at typical junctions using 2D analyses with an equivalent span, defined as the diagonal length across the junction. This equivalent span approach is widely used in assessing tunnel junction behaviour between mainline tunnels and cross passages, yet there is limited comprehensive qualitative analysis assessing it.

This study first explores tunnel junction displacement under various conditions to identify relationships between key variables such as tunnel span, geological conditions, ground cover, and tunnel orientation. A series of 3D numerical analyses were conducted using FLAC3D (finite difference program), and these results were then compared with those from 2D analyses using RS2 (finite element program) that applied the equivalent span method. The study provides new insights and guidance on the equivalent span approach, with findings confirming that 2D modelling, when adjusted based on insights from 3D modelling, can effectively support the design of tunnel junctions.

1. INTRODUCTION

Tunnel junctions, where main tunnels intersect with access tunnels or substations, present engineering challenges due to their complex geometry, additional free surfaces, and increased support requirements. These junctions often experience elevated displacements during construction, necessitating additional design and support measures. Although 3D modelling offers detailed insights into junction displacement and stress redistribution, it is typically reserved for critical scenarios due to its time-consuming nature. 2D numerical modelling is commonly used to evaluate displacements and tunnel support performance for standard junction designs, such as cross passages or adits.

Previous studies, such as those by Hsiao et al. (2009), have advanced our understanding of tunnel junction behaviour, particularly in estimating crown displacements under varying conditions. Based on extensive numerical simulations, their work highlighted the effects of in situ rock mass strength-to-stress ratio and intersection angles on tunnel displacements.

In recent tunnel projects in Sydney, a simplified method has been adopted to estimate displacement and support performance at typical junctions using 2D analyses. This method uses an equivalent span defined as the diagonal length across the junction (Figure 1). The equivalent span approach is widely used to assess tunnel junction behaviour between mainline tunnels and cross passages. While the primary justification for this method often cites its successful application in previous projects, there is limited comprehensive qualitative analysis to support its effectiveness. As a young tunnel engineer, the author is particularly intrigued by this approach to junction design and decided to pursue this assessment to gain deeper insights.

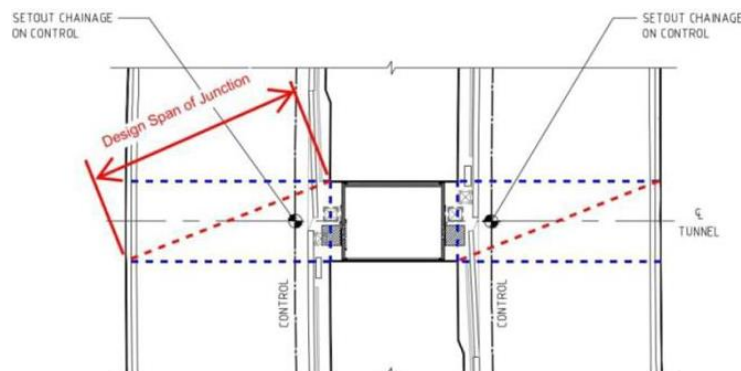


Figure 1: Effective span approach

1.1 STUDY OBJECTIVES

The broader implications of the equivalent span approach, especially across varying ground conditions and tunnel orientations, have not been extensively explored. This study is divided into two parts to understand the equivalent span method better:

- **3D Numerical Analyses Using FLAC3D:** The first part involves conducting a series of 3D numerical analyses using FLAC3D. By systematically varying parameters such as tunnel span, ground conditions, ground cover, and tunnel orientation, the assessment aims to understand tunnel displacement behaviour under different conditions.
- **Comparison with Equivalent Span 2D Analyses:** This part compares the displacement results from the 3D analyses with those obtained using equivalent span 2D finite element analysis (FEA) conducted with RS2, a finite element program developed by Rocscience. The objective is to compare the results to identify trends or relationships and evaluate the adequacy of the equivalent span approach.

Building on the framework established by Hsiao et al. (2009), this study expands to include different mainline and access tunnel spans and incorporates parameters to simulate typical tunnelling conditions within the Sydney Hawkesbury Sandstone.

2. NUMERICAL ASSESSMENT

2.1 ROCK MASS PROPERTIES

Parameters and classifications for Sydney sandstone and shale in tunnel projects are detailed by Pells (2002) and Bertuzzi (2014). It is well-documented that Hawkesbury sandstone experiences significant horizontal in-situ stresses. The in-situ stress relationships proposed by Oliveira and Parker (2014) model the major horizontal stress (σ_H) as a function of the vertical stress (σ_v) for different rock mass stiffness, with the minor horizontal stress (σ_h) being $0.61 \cdot \sigma_v$. These relationships are adopted in this numerical assessment.

Oliveira and Diederichs's study (2017) highlighted the brittle nature of Hawkesbury sandstone, which is characterised by tensile cracking and fracture propagation under high in-situ stress conditions. Table 1 presents the block-scale brittle model parameters for sandstone, including the properties of joints and beddings derived from previous tunnel projects in Sydney, which were adopted in the 2D FEA

Table 1: Rock parameters adopted for discontinuum modelling (block scale parameters)

Geotechnical Parameters for Sandstone		SS-II	SS-III		
Intact Rock Parameters	UCS (MPa)		25	12	
	Poisson's Ratio		0.25		
	Bulk Unit Weight (kN/m ³)		24		
	Hoek Brown - m_i		17		
Block scale or Discontinuum Approach	Rock Mass Modulus E_{mass} (MPa)		4,500	2,500	
	Generalised Hoek-Brown	GSI_{peak}		90	90
		$GSI_{res}^{(2)}$		27	27
		Brittle model – peak strength	mb	1.556	
			s	0.09151	
			a	0.25	
		Brittle model – residual strength	mb	12	
			s	0.0001	
	a		0.75		
	Dilation Parameter		0.75		
Bedding	Average spacing (m)		1	0.5	
	Normal Stiffness K_n (MPa/m)		4000		

Geotechnical Parameters for Sandstone		SS-II	SS-III
	Shear Stiffness K_s (MPa/m)	400	
	JCS (MPa)	25	12
	JRC	6	4
	Res. Friction angle ($^\circ$)	32	
Joint	Average spacing (m)	2	1
	Normal Stiffness K_n (MPa/m)	8000	4000
	Shear Stiffness K_s (MPa/m)	800	400
	JCS (MPa)	25	12
	JRC	8	6
	Res. Friction angle ($^\circ$)	40	

An elastic transversely isotropic behaviour was simulated in the 3D elastic continuum analyses to capture the effect of the discontinuities within the rock mass. This was characterised by a ratio of 10 between the maximum displacement modulus and the shear modulus (E/G) (Oliveira & Wong, 2012), with the specific values presented in Table 2.

Table 2: Rock parameters adopted for the 3D equivalent continuum modelling

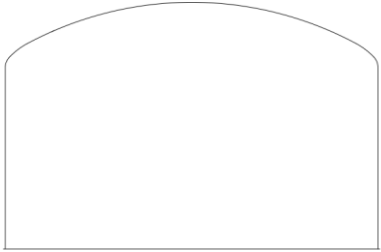
Rock Mass	Young's Modulus (MPa)	Vertical Young's Modulus (MPa)	Horizontal Young's Modulus (MPa)	Shear Young's Modulus (MPa)
SS-II	2000	1333	4000	200
SS-III	1000	667	2000	100

2.2 ASSESSMENT VARIABLES

The numerical study systematically evaluated tunnel junction performance using key variables outlined in Table 3. Two ground cover depths (20 and 40 meters) were analysed to represent typical conditions in Sydney's tunnelling projects. Intersection angles of 90° and 60° were considered to assess symmetrical and asymmetrical junctions. The study included four mainline tunnel spans (12, 14, 16, and 20 meters) and four access tunnel spans (6, 8, 10, and 12 meters), all with a height of 8 meters. The mainline tunnel extended 100 meters, while the access tunnel extended 40 meters. The tunnel profile adopted is a typical Sydney flat roof tunnel profile as shown in Figure 2.

A total of 42 cases combining these variables were assessed in FLAC3D to investigate tunnel junction behaviour under various conditions.

Table 3: Tunnel conditions considered in the study

Rock Mass	Sydney Hawkesbury Sandstone SS-II Sydney Hawkesbury Sandstone SS-III
Ground Cover (m)	20m 40m
Intersecting Angle ($^\circ$)	90, 60
Tunnel Profile	 <p style="text-align: center;">Figure 2: Typical Sydney flat roof tunnel profile</p>

Mainline tunnel span, T_M (m)	12m,14m,18, 20m
Access tunnel span, T_A (m)	6m,8m, 10m,12m
Mainline and access tunnel height (m)	8m
Mainline tunnel length(m)	100m
Access tunnel length(m)	40m

2.3 FLAC3D MODEL SET UP

Figure 3 illustrates the model set-up for 2 cases in FLAC3D, primarily demonstrating the model layout and mesh configurations used in the simulations. The model boundaries were set at three times the maximum mainline tunnel span in both the x and y directions and three times the tunnel height in the negative z direction. This boundary condition minimises the influence of boundary effects on the modelling, ensuring an accurate representation of stress and displacement behaviours within the tunnel environment.

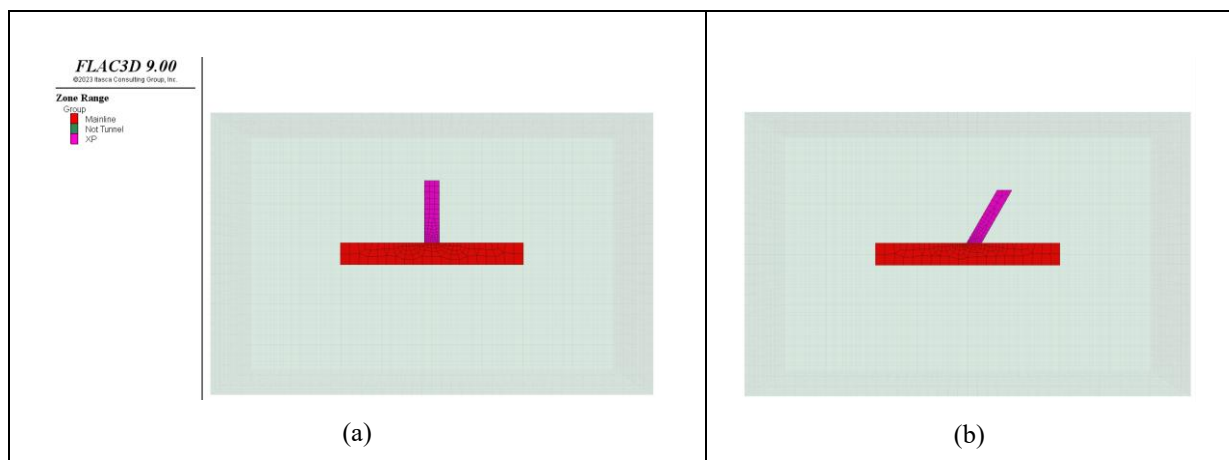


Figure 3: FLAC3D models for different intersection angles: (a) 90° (b) 60°

3. 3D ANALYSES RESULTS AND ASSESSMENT

To gain insights into the relationships between variables, displacement contours and stress distributions were assessed through long sections, plan views, and cross-sections (Figure 4 and Figure 5 for reference). This comprehensive analysis aimed to understand displacement behaviour and stress variations within the tunnel environment. The following sections present the key takeaways from this assessment.

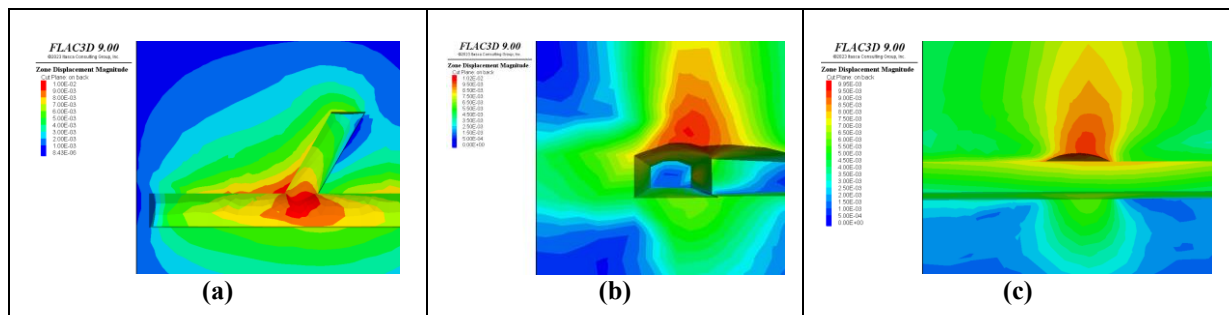


Figure 4: FLAC3D displacement contours: (a) Plan view of tunnel roof displacement (b) Cross section (c) Longitudinal section

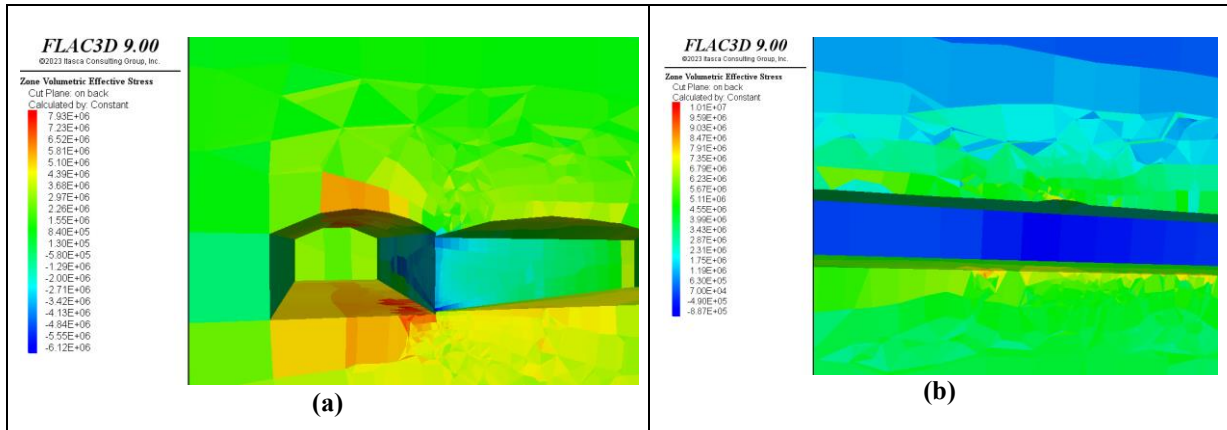


Figure 5: FLAC3D stress contours: (a) Plan view (b) Cross section (c) Longitudinal section

3.1 RATIO OF MAINLINE TO ACCESS TUNNEL SPAN ($\frac{T_m}{T_a}$)

Figure 6 shows the relationship between additional mainline roof displacement due to the access tunnel ($\frac{D_m}{D_{m0}}$) and $\frac{T_m}{T_a}$ ratios. Key findings are:

- **Displacement Trend:** $\frac{D_m}{D_{m0}}$ peaks at around 30 to 45% when $\frac{T_m}{T_a}$ is 1. As $\frac{T_m}{T_a}$ increases to 2, $\frac{D_m}{D_{m0}}$ decreases to approximately 15%.
- **Model Fit:** A logarithmic model ($R^2 = 0.82$) better captures this relationship than a linear model ($R^2 = 0.75$).

For Sydney road tunnels, the mainline tunnels generally span 12-16 meters, with cross passages around 6-8 meters. This indicates that $\frac{D_m}{D_{m0}}$ ranges from 25% to 15%. For ventilation tunnels, the ratio can be as low as 1, requiring additional support due to higher displacement. These findings assist in providing an initial displacement estimation based on known $\frac{T_m}{T_a}$.

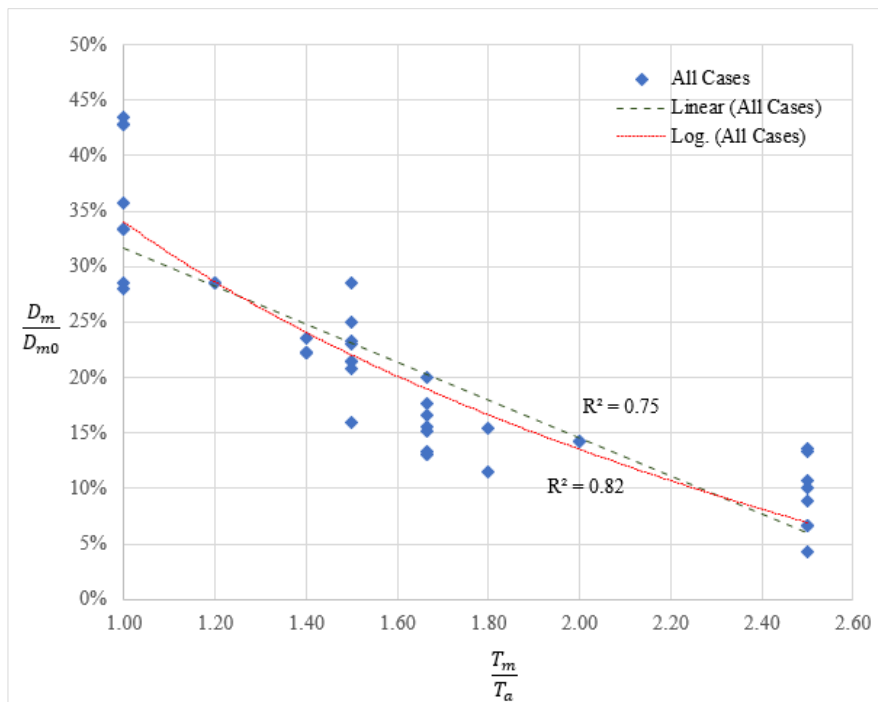


Figure 6: Relationship between $\frac{D_m}{D_{m0}}$ and $\frac{T_m}{T_a}$

3.2 RATIO OF UCS TO FIELD STRESS ($\frac{\sigma_{cm}}{P_0}$)

The ratio of the uniaxial compressive strength (UCS) of the rock mass to the maximum in situ stress, a key factor influencing tunnel stability (Hoek, 1998), was assessed against $\frac{D_m}{D_{m0}}$. Table 1 details the UCS values of the rock mass, while the maximum field stress values were derived from FLAC3D analyses. Figure 7 illustrates the relationship between $\frac{D_m}{D_{m0}}$ and $\frac{\sigma_{cm}}{P_0}$.

The analysis shows that increasing the $\frac{\sigma_{cm}}{P_0}$ ratio has minimal effect on additional roof displacement across all analysed cases, as they all have $\frac{\sigma_{cm}}{P_0}$ values greater than 1.0. This aligns with the findings of Hsiao (2009), who noted that the percentage of additional roof displacement changes minimally when $\frac{\sigma_{cm}}{P_0}$ exceeds 0.5.

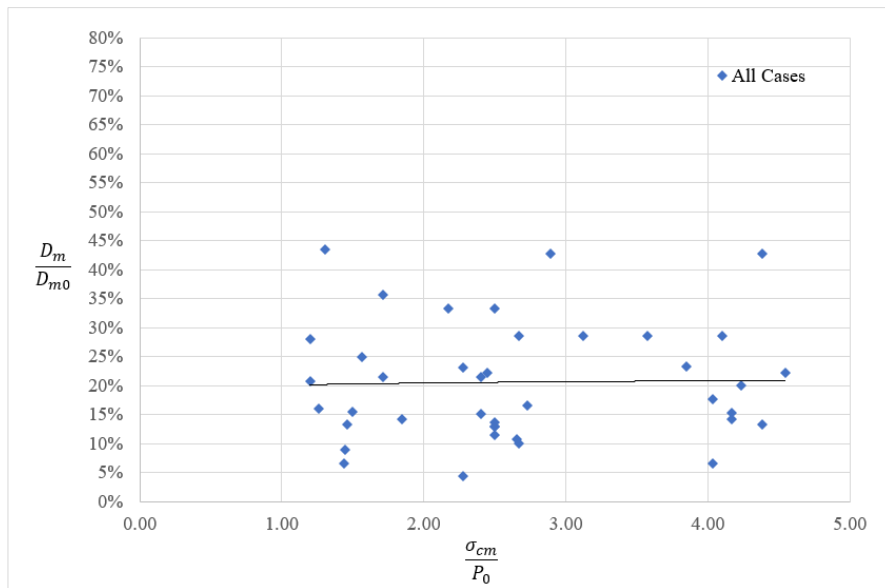


Figure 7: Relationship between $\frac{D_m}{D_{m0}}$ and $\frac{\sigma_{cm}}{P_0}$

3.3 ZONE OF INFLUENCE

Tunnel crown displacement contours for each case were qualitatively analysed to assess the zone of influence. As anticipated, 90° junctions exhibit symmetrical displacement contours, with the highest displacement concentrated directly above the junction and gradually decreasing outward. The 60° junctions display asymmetrical contours, with higher crown displacement observed towards the acute angle.

Figure 8 The tunnel crown displacement for 90-degree and 60-degree junctions is illustrated for reference from a specific case.

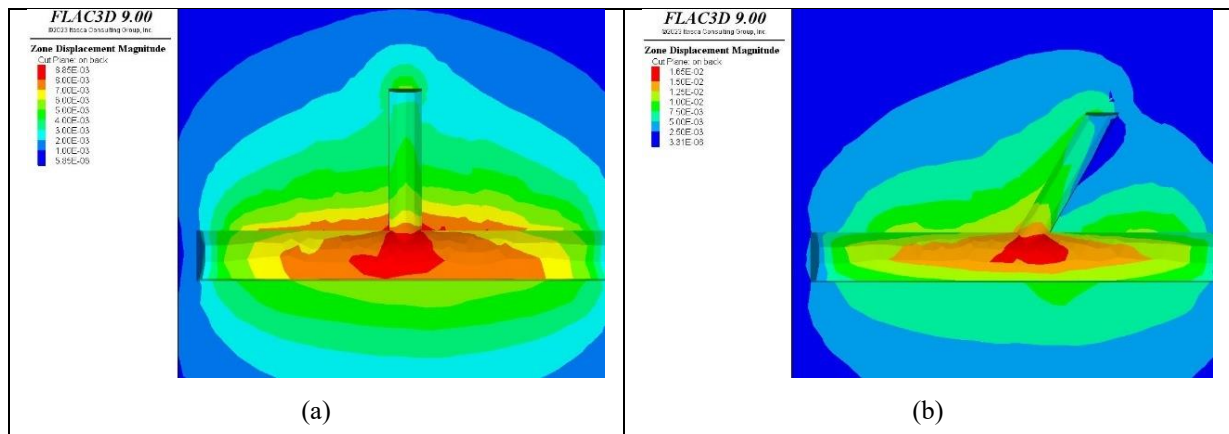


Figure 8: Plan view of tunnel roof displacement: (a) 90° junction (b) 60° junction

To further quantify the zone of influence, two plots were generated for 90° and 60° junctions (Figure 9), the Y-axis represents the $\frac{T_m}{T_a}$ ratio, while the X-axis represents the extent of the zone of influence, measured as the distance from the tunnel junction centre where displacement reaches 80% of the maximum value.

This assessment focuses on $\frac{T_m}{T_a}$ ratios less than 2, as Section 3.2 indicates that when the ratio exceeds 2, excavation of the access tunnel only induces an additional settlement of around 10-15% on the mainline, translating to 1-4 mm, which has a negligible impact on ground support.

The analysis shows that the zone of influence increases with the $\frac{T_m}{T_a}$ ratio for both SS-II and SS-III rock masses. Specifically:

- 90° junctions demonstrate a more linear and consistent increase in the zone of influence, ranging from about 10 m to 30 m as the $\frac{T_m}{T_a}$ ratio increases from 1 to 1.8.
- 60° junctions show a greater zone of influence towards the acute angle side, indicating asymmetrical displacement patterns.

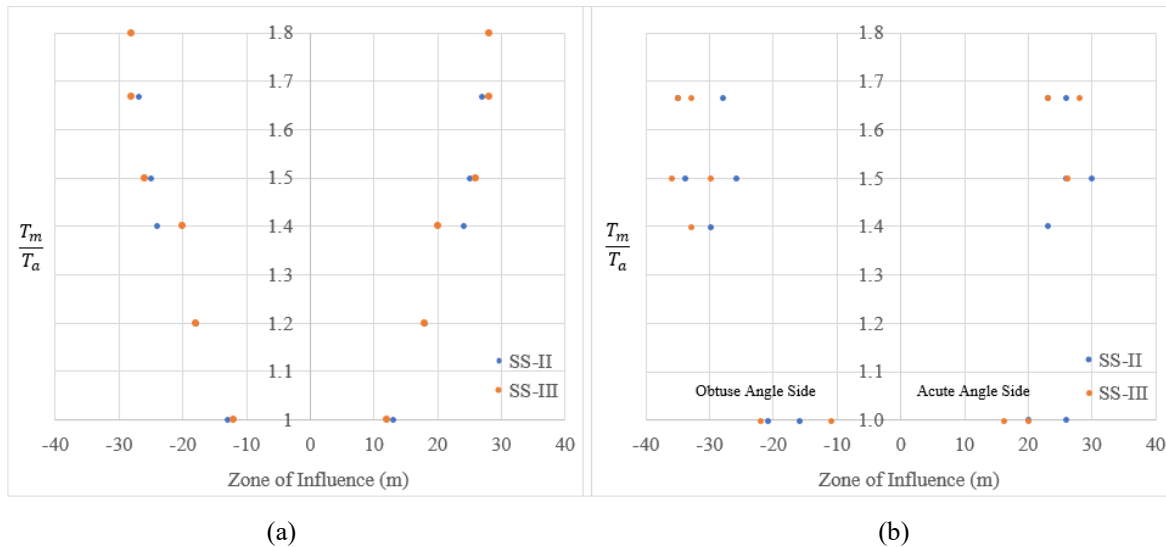


Figure 9: Zone of Influence: (a) 90° junction (b) 60° junction

4. COMPARATIVE ANALYSIS OF 2D AND 3D RESULTS

This section compares the results of 3D FLAC3D simulations and 2D RS2 models adopting an equivalent span approach, the analysis was carried out for cases with $\frac{T_m}{T_a}$ ratio less than 2.

4.1 2D MODEL SET-UP

The equivalent span for each case was determined based on the diagonal length across the tunnel junction. This span was then modelled in RS2. The rock mass was modelled as an elastic-plastic discontinuous material, adopting the Generalised Hoek-Brown failure criterion with parameters outlined in Table 1. Both sets of analyses used consistent surcharge and boundary conditions. Figure 10 presents the model setup in RS2.

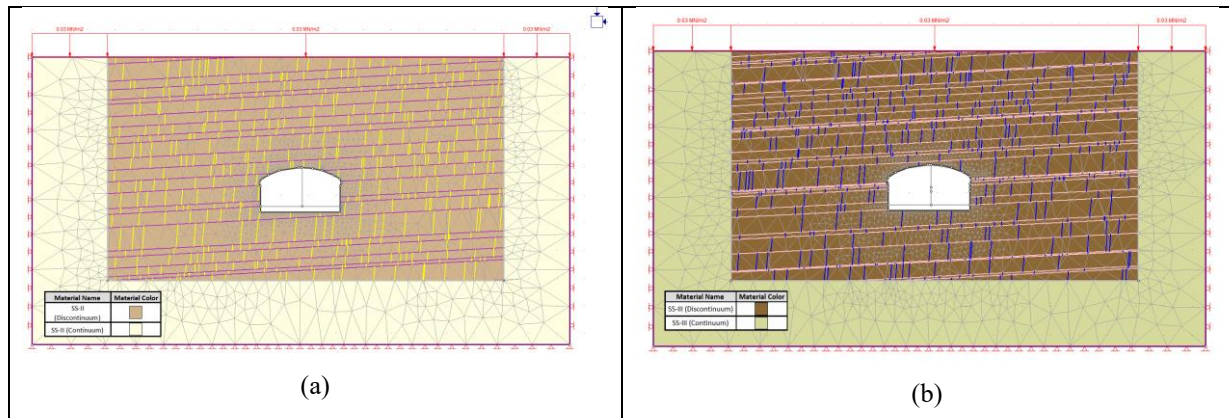


Figure 10: 2D analysis model set up (a) SS-II (b) SS-III

4.2 COMPARISON OF DISPLACEMENT

Figure 11 presents the ratio of 2D to 3D displacements ($2D/3D$) across different equivalent spans.

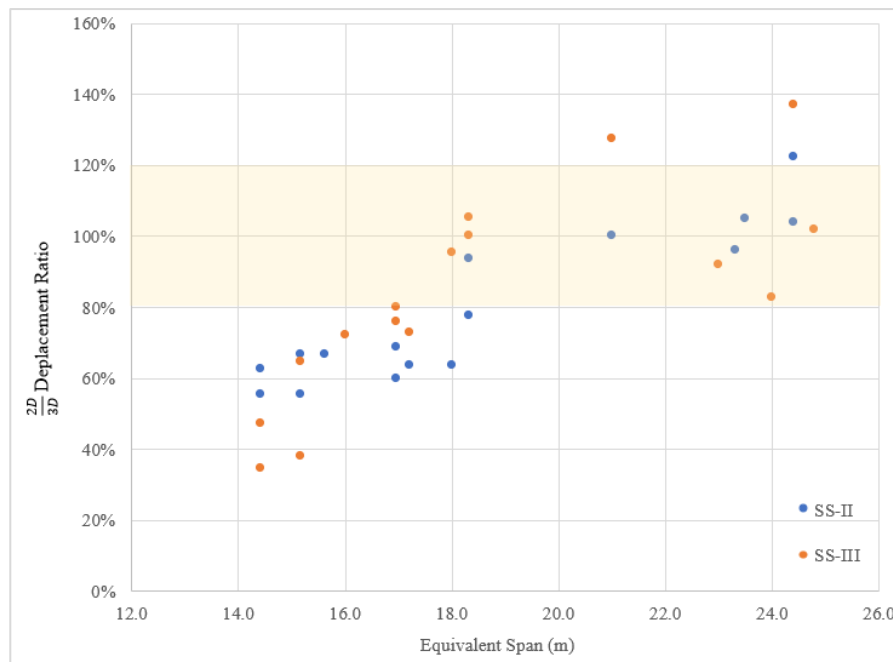


Figure 11: Ratio of 2D to 3D displacements ($2D/3D$) across different equivalent spans

Key observations include:

- **Spans around 14-16m:**
 - 2D models adopting an equivalent span cross-section estimated displacement at typically 50-70% of what was observed in 3D models. Stress redistribution and interactions are more localised and intricate for smaller spans, especially in SS-III, which is more heavily jointed. The higher frequency of joints and discontinuities in SS-III means that the discontinuities affect the stress distribution greatly. These interactions are not fully accounted for in 2D models, as they assume plane strain conditions and do not capture the complex three-dimensional stress paths. Consequently, for smaller spans, the estimated values from 2D models for SS-III deviate even further from the 3D models compared to SS-II
- **Spans greater than 18 m:**
 - For spans greater than 18 meters, the results from the 2D models align more closely with those from the 3D models, with deviations generally within $\pm 20\%$. This suggests that the 2D model can reasonably approximate the 3D behaviour, considering the inherent variability in numerical modelling outcomes, such as differences in mesh density, element type, and boundary conditions.

In larger spans, stress distribution and deformation tend to average over a broader area, reducing the significance of localised effects. The averaging effect over broader areas in larger spans allows the 2D models to approximate the 3D behaviour better, resulting in more accurate and comparable displacement predictions.

4.3 COMPARISON BETWEEN SS-II AND SS-III

- **SS-II:** The data points for SS-II are more concentrated, indicating a higher degree of predictability and consistency due to its homogeneous nature.
- **SS-III:** The data points display more variability in results, although it aligns well with 3D models for spans greater than 18 meters. SS-III is weaker and less homogeneous, leading to more scattered data points and greater variability in deformation patterns.

4.4 IMPLICATIONS AND RECOMMENDATIONS

This comparative analysis suggests introducing a span adjustment factor to better align 2D representations with 3D results. However, making this approach more robust requires considering additional variables, such as angle adjustment factors and specific geological conditions. The impact of intersection angles on stress distribution and displacement behaviour, as observed in 90° and 60° intersections, indicates that angle adjustments are important for a comprehensive assessment.

Recognising the limitations of 2D models, the use of 3D simulations is recommended for more complex junctions or when higher accuracy is required. Continuous validation and calibration of the 2D models against 3D results and field data will enhance the reliability of the equivalent span approach. By integrating these adjustments and validations, engineers can improve the accuracy of 2D models, ultimately supporting safer and more efficient tunnel designs. Future studies should continue to refine these methods and validate them across various conditions to ensure their robustness and applicability in different tunnelling scenarios.

CONCLUSION

The 3D analyses highlighted that the mainline-to-access tunnel span ratio ($\frac{T_m}{T_a}$) is a key factor in influencing displacement. The displacement ratio ($\frac{D_m}{D_{m0}}$) peaks when the $\frac{T_m}{T_a}$ ratio is around 1, showing the highest additional displacement when the spans are equal. As the $\frac{T_m}{T_a}$ increases to 2, the displacement ratio decreases, indicating that larger mainline spans relative to access tunnels mitigate additional displacement effects. These findings underscore the importance of considering $\frac{T_m}{T_a}$ ratios in assessing displacement behaviour at tunnel junctions.

Comparative analyses between 3D and 2D models provided insights into the effectiveness and limitations of the equivalent span approach. For smaller spans (14-16m), 2D models are observed to underestimate displacements, especially in homogeneous rock masses like SS-II. However, for larger spans (over 18 meters), 2D and 3D results aligned more closely, with deviations generally within $\pm 20\%$. This suggests that 2D models can approximate 3D behaviour for larger spans, but they require span adjustments for smaller spans to account for localised stress redistributions and interactions.

Improving the applicability of the equivalent span approach relies on continuous validation and calibration of 2D models against 3D results and field data. This study lays the groundwork for further investigations in varying ground conditions, such as shale, and explores additional variables, including different tunnel shapes and rock mass properties; future research could delve deeper into assessing tunnel shape and intersection angle adjustment factors.

5. ACKNOWLEDGEMENT

I want to express my sincere gratitude to my colleagues at AECOM, Arun Sarathchandran and Jaden Chow, for their thorough review, insightful advice, and readiness to answer my questions. I am also deeply thankful to Ali Goshani for his support throughout the development of this paper and to Arjun Shivasami for taking the time to review it. Your support and encouragement have meant a lot to me. This journey has been a wonderful opportunity to grow my technical writing skills and deepen my understanding of the subject. Thank you all for being a part of it.

6. REFERENCES

- Bertuzzi, R., 2014. Sydney sandstone and shale parameters for tunnel design. *Australian Geomechanics Journal*, 49(1), pp.95-104.
- Hoek, E., (1998). Tunnel support in weak rock. Keynote address, Symp. on Sedimentary Rock Engineering, Taipei, Taiwan, p. 20-22 October.
- Hsiao, F.Y., Wang, C.L. and Chem, J.C., (2009). Numerical simulation of rock displacement for support design in tunnel intersection area. *Tunnelling and Underground Space Technology*, 24(1), 14–21.
- Oliveira, D.A.F. and Diederichs, M.S., 2017. Tunnel support for stress induced failures in Hawkesbury Sandstone. *Tunnelling and Underground Space Technology*, 64, pp.10-23.
- Oliveira, D.A.F. and Parker, C.J., 2014. An alternative approach for assessing in situ stresses in Sydney. In: *Proceedings 15th Australasian Tunnelling Conference*. Melbourne: The Australasian Institute of Mining and Metallurgy, pp.189-194.
- Oliveira, D.A.F. and Wong, P., 2012. Selection of rock mass design parameters for assessing excavation induced movements in the Sydney CBD. In: *Proc.: ANZ 2012 Conference*.
- Pells, P.J.N., (2002). Developments in the design of tunnels and caverns in the Triassic rocks of the Sydney region. *International Journal of Rock Mechanics and Mining Sciences*, 39(5), 569–587.